Applied Thermal Engineering 248 (2024) 123267

Contents lists available at ScienceDirect

Applied Thermal Engineering

journal homepage: www.elsevier.com/locate/apthermeng

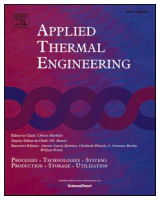

Research Paper

Validation of a calibrated steady-state heat network model using measured data

Diana Maldonado [a,*], Patrik Schönfeldt [a], Herena Torio [a], Francesco Witte [a], Michael Füting [b]

[a] Institute of Networked Energy Systems, German Aerospace Center (DLR), Carl-von-Ossietzky-Str. 15, Oldenburg 26129, Germany
[b] Institute of Space Propulsion, German Aerospace Center (DLR), Im Langen Grund, Hardthausen 74239, Germany

ARTICLE INFO

Keywords:
District heating system
Calibration and optimisation
Temperature simulation
Thermal engineering systems in python (TESPy)

ABSTRACT

Expanding and modernizing District Heating (DH) systems in cities is a concrete way to foster the decarbonization of the heating sector. Therefore, methods that allow for faster and accurate simulations when limited information about the network is available are required. This paper proposes a method for employing a steady-state model with relatively low computational effort, enabling the creation of a rather coarse model of a heating network. This model is parameterised by making assumptions about the network's topology and pipe characteristics. Later, the model is calibrated using a heuristic approach, in which the combination of the heat transfer coefficient and the length parameters of each pipe in the network are selected as the calibration target vector, meaning that these initial assumptions of the network are no longer required. The approach is validated using measured data from a specific case study and compares the results of the uncalibrated model with those of a calibrated one. After calibration, the model was found to obtain a mean absolute temperature error below 0.5 °C.

1. Introduction

According to the International Energy Agency's (IEA) 2023 heating report, space and water heating accounted for about half of the world's energy demand for buildings in 2021 [1]. Furthermore, 60 % of this heating demand is met by the combustion of fossil fuels [1]. In Germany, the space heating and hot water demand alone consumed 34 % of the country's total final energy consumption, with a total of 770 TWh in 2020 [2,p. 11]. In contrast to the liberalised electricity sector, the heating demand belongs to the least decarbonised sectors, with only 14 % supplied by renewable energies (RE) [3,4,5]. Local governments and states are looking for solutions for this sector, and district energy networks, which refers to connecting local resources to local needs, can be one of them [6].

District heating (DH) systems are widely used to meet heating, hot water and cooling demands through a network of insulated pipes [7]. Expanding and modernising DH systems in cities is a concrete way to drastically reduce fossil fuels consumption and foster the acceleration of the decarbonisation in the heating sector [6,8], as they are suited to feed in locally available, renewable and low-carbon energy sources, such as solar thermal and geothermal heat and waste heat from industry and commercial buildings.

DH systems are categorised by Lund et al. based on the heat carrier, i.e. the temperature delivered and the pressure level, dividing them into the so-called generations of DH systems [9,10]. The first two generations used steam and pressurised hot water as the main heat carriers. In the third generation, pressurised water is still the heat carrier, but the flow temperatures are often below 120 °C. Typical features of these systems are underground insulated pipes and are still widely used [9]. A clear trend towards lower distribution temperatures has triggered the fourth and fifth generations of DH system. These new generations are focused on energy efficiency, smart integrated energy systems, the use of locally available renewable energy sources, and operating temperatures closer to the temperature of the actual heat demand in order to minimise thermodynamic losses. Furthermore, the later one triggers a step forward to the combination of heating and cooling [10]. These latter two generations have the overarching aim of decarbonisation in common.

Despite the efforts to introduce the new generations of DH systems, the sector is still dominated by the third generation. For instance, Germany's dominant technology for the DH provision is combined heat and power (CHP), plants with a share of 86 % and only 14 % for other technologies [5,11]. In these systems, heat is usually delivered at temperatures between 70 °C and 120 °C. The substitution of heat supply technologies with renewable heat supply systems, such as solar thermal

* Corresponding author.
E-mail address: diana.maldonado@dlr.de (D. Maldonado).

https://doi.org/10.1016/j.applthermaleng.2024.123267
Received 21 September 2023; Received in revised form 23 April 2024; Accepted 24 April 2024
Available online 25 April 2024

or heat pumps, is accompanied by a reduction in temperature. While this reduces heat losses in the heating network, it also has a direct impact on the final delivery to the consumer, requiring adjustments to the domestic heating system. In order to select appropriate heating supply technologies, simulating the response of DH networks to potential changes in operating conditions is a crucial task. Therefore, methods that allow faster and accurate simulations when limited information of the network is available, are required to help to modernize these systems.

1.1. Modelling heat networks

Network modelling is fundamental for simulating the response of DH systems to changes in operating conditions [7,12]. Transient and steady-state simulations are two common approaches to modelling physical heat networks. Transient simulations, also known as dynamic simulations, are used to model heating networks under varying conditions and consider thermal inertia of the system. In contrast, steady-state simulations are used to model heating networks under relatively constant thermal conditions over time. The selection of an appropriate modelling approach depends on the generation of the system, the availability of data and the purpose of the analysis.

Since the development of cheaper and faster computers, dynamic simulations for the operation of DH systems have often been performed e.g., Benonysson [13], Bohm [14], Larsen et al. [15,16], Gabrielaitiene [17], Stevanovic [18], Van der Heijde et al. [19] among others. One of the main differences between the two simulation approaches is that dynamic simulations are able to represent the thermal inertia of the DH system by differential equations. Guelpa [12] analysed the importance of including the thermal behaviour of the network (e.g., thermal losses, thermal transients and delay time) in the analysis of DH operations. The analysis highlights, that the thermal transients should be considered in the following two main cases: 1) large networks i.e., distances from 1000 to 2000 m to the consumers and diameters from 200 to 800 mm. 2) significant fluid cooling in some parts of the network, triggered by changes in mass flow (e.g., night shutdown or setback). Similar results were found by Sartor & Dewakef [20] and described by Brown et al. [7], whereby the thermal inertia of the pipe has a significant effect on the pipe's outlet temperature response, particularly when rapid temperature changes occur, such as the morning boost of the network. However, the fluid dynamic problem of DH pipelines is non-linear and this is usually solved by numerical methods which are often computationally expensive [7]. Therefore, in order to reduce the efforts of dynamic simulations, steady-state simulations and simplifications of the network structure are used to simulate the network at considerably reasonable levels of accuracy [21].

Steady-state analysis are described by Benonysson [13], Wallentén [22], Duquette [23] among others. Van der Heijde et al. [24], presented the mathematical derivations for the steady-state heat losses in double pipes, whereby the total heat losses calculated with the developed model were found to be in accordance with the nominal values provided by the manufacturer. It was also found that under certain operating conditions, e.g., relatively high mass flows and temperatures below 100 °C [24], steady-state models are suitable for the analysis, which includes the simplification of the energy and continuity equation by deleting the negligible terms such as axial heat diffusion, pressure difference energy and wall friction dissipation. Wang et al. [25] presented a matrix steady-state simulation model based on a DH system configuration simplified to two basic elements (branches and nodes). Due to the uncertainty of some model parameters, the differences between predicted and observed temperature required calibration before obtaining useful results from the simulation. A non-aggregated steady-state model is proposed by Wang [21] to estimate on-site heat losses of a typical pipe network with hourly measurements of heat sources and several substations. A detailed heat loss profile along each pipe can be obtained by the proposed model, which can significantly improve the accuracy of locating damaged insulation.

To date, there are many tools available to analyse DH networks using a steady-state approach. Some of them are designed for specific cases, such as the creation and optimisation of new DH networks presented by DHNx [26,27], the analysis of double thermal networks by DiGriPy [28] or the analysis of new district heating and cooling systems (5th generation) by nPro [29]. There are some others that are more flexible in terms of system coupling and design such as TESPy [30] and Pandapipes [31]. All of these tools require information on pipe characteristics, topology and thermal behaviour. However, the question arises how to model systems in case not all the information normally required is available.

Therefore, the aim of this work is to present a methodology for modelling and calibrating a steady-state DH network when limited information about the network is available. The method proposes that employing a steady-state model with relatively low computational effort, enables the creation of a rather coarse model of a heating network, which describes the topology, and parameterise it using a heuristic approach. The method is validated using measured data from a specific case study and comparing the results of an uncalibrated model with a calibrated one. The uncalibrated model makes assumptions about the network topology and the pipes' characteristics, such as distance and heat transfer coefficients. For the calibrated model, measurement data for temperature and heat demand are used to modify the assumptions made in the uncalibrated model in order to minimise the difference between the measurements and the model's prediction.

Based on such model, it will be possible to conduct a variety of analyses in future research, for example, to investigate the effect of reduced supply temperature or decentralised heat production on the network. The following are the main contributions of this paper:

1. A method for building a steady-state DH model using a multi-objective function to parameterise and calibrate it. Compared to a normal calibration based on manufacturer's values, the proposed calibrated model's prediction of the thermal behaviour of the network is improved.
2. By considering the length, heat transfer coefficient and diameter of each pipe as a single term for heat losses calculations, the proposed calibration proves its effectiveness as a method to be used when limited information on pipe characteristics is available.

The remaining part of this paper is organized as follows. In Section 2, the governing equations of the thermodynamic model are described. Next, a method for calibrating the thermodynamic model representing an existing district heating network is developed in Section 3, using various technical parameters and measured data of this system. The proposed method is tested using a case study of the Lampoldshausen district heating network. In Section 5, the main findings are presented, including the results and validation of the thermodynamic model. Finally, the conclusions and outlook of the research are presented in Section 6.

2. Thermodynamic model

As presented in Section 1.1, there are several models and methods for representing the thermal behaviour of a DH network. Typically, mass balance and energy balance equations are used to model the steady-state operation of a DH system. Optionally, the hydraulic state can be determined, but it is not the first priority for thermal network modelling. Therefore, the hydraulic state of the system is neglected in this study.

For each component of the network, the total mass flow entering must be equal to the total mass flow leaving as seen in Eq. (1). The energy balance of all components can be derived from the stationary energy balance of open systems with multiple inlets and outlets (Eq. (2)). The rate of heat $\dot{Q}$ and power $\dot{W}$ transferred, depend on the properties of the individual components: for example, the pipes of the system and the

heat demand representation do not transfer power, thus the value of $\dot{W}$ is equal to zero. A control valve or a merge point transfers neither power nor heat, therefore both $\dot{Q}$ and $\dot{W}$ are equal to zero.

$$0 = \sum_i \dot{m}_{\text{in},i} - \sum_i \dot{m}_{\text{out},i} \tag{1}$$

$$0 = \sum_i \dot{m}_{\text{out},i} \cdot h_{\text{out},i} - \sum_i \dot{m}_{\text{in},i} \cdot h_{\text{in},i} - \dot{W} - \dot{Q} \tag{2}$$

For junctions that separate branches, the energy balance equation alone is not sufficient because the temperature of all of their outlets must be equal to the inlet temperature value (Eq. (3).

$$0 = T_{\text{in}} - T_{\text{out},k} \;\forall\; k \in \text{outlets} \tag{3}$$

Different branches in a district heating system can be decoupled hydraulically by using heat exchangers. A heat exchanger that transfers heat from one medium to a different medium is often considered to be adiabatic to the ambient, thus all the heat delivered from the hot side is provided to the cold side of the heat exchanger, resulting in the energy balance equation, depicted in Eq. (4).

$$0 = \dot{m}_{\text{out,hot}} \cdot \left(h_{\text{out,hot}} - h_{\text{in,hot}}\right) + \dot{m}_{\text{out,cold}} \cdot \left(h_{\text{out,cold}} - h_{\text{in,cold}}\right) \tag{4}$$

The rate of heat transferred $\dot{Q}$ can also be expressed as a function of the inlet and outlet temperatures by the logarithmic temperature difference $\Delta T_{\log}$ (in K) and the heat exchangers' properties, i.e. the heat transfer coefficient U (in W/m^2 K) and the effective heat transfer area A (in m^2) in Eq. (5). The heat transfer coefficient generally depends on the flow regimes on both sides as well as the materials used. The logarithmic temperature difference is defined, for example for a counter-current heat exchanger in Eq. (6).

$$\dot{Q} = U \cdot A \cdot \Delta T_{\log} \tag{5}$$

$$\Delta T_{\log} = \frac{T_{\text{out,hot}} - T_{\text{in,cold}} - \left(T_{\text{in,hot}} - T_{\text{out,cold}}\right)}{\ln \frac{T_{\text{out,hot}} - T_{\text{in,cold}}}{T_{\text{in,hot}} - T_{\text{out,cold}}}} \tag{6}$$

This relation can be transferred to the modelling of the network's pipes in order to calculate their heat loss during operation: the pipes are the hot side of the heat exchanger, the surrounding subsurface is the cold side of the heat exchanger. Pipe parameters are typically obtained through physical measurements and supplemented with technical specifications provided by the manufacturer or network designer. Also, literature (e.g. Nussbaumer [32]) provides methods to calculate the U value of pipes buried in the subsurface. However, these methods require technical details about the pipes, for example the material of the pipe, insulation, distance between feed and return flow pipes and the size of each layer. Information on the surrounding medium (e.g. soil or air) and the flow regime is also required [32]. Especially for existing systems, this information is not necessarily available.

Therefore, a more simplified approach is suggested instead: the term $K = U \cdot A$ (the product of heat transfer coefficient and heat transfer area) is introduced. The K value of the relevant pipes can be adjusted in a model in a way that the model accurately predicts measurement data, e.g. the temperature at the outlet of a pipe based on a known inlet temperature and mass flow. For that, an assumption regarding the soil temperature is required to calculate the logarithmic temperature difference between the pipe and the soil. If the fluid temperature inside the pipe does not change significantly (e.g. in short pipe sections or with low temperature difference between fluid and soil temperature), the soil temperature can be assumed constant along the length of the pipe.

With this approach Eq. (6) can be simplified to Eq. (7) and the heat losses of the pipe are calculated according to Eq. (8).

$$\Delta T_{\log,\text{pipe}} = \frac{T_{\text{in}} - T_{\text{out}}}{\ln \frac{T_{\text{in}} - T_{\text{soil}}}{T_{\text{out}} - T_{\text{soil}}}} \tag{7}$$

$$\dot{Q}_{\text{pipe}} = K \cdot \Delta T_{\log,\text{pipe}} \tag{8}$$

3. Methodology

This section describes the approach taken to collect the necessary data from the DH network, build the thermodynamic model, calibrate it with a subset of measured data and finally validate it. These three steps are explained in detail in sections 3.1, 3.2 and 3.3 respectively.

3.1. Model parameterisation

Collecting accurate data is fundamental to building an effective heat network simulation. Without comprehensive and reliable data on the characteristics of the network, the simulation model may not accurately represent the behaviour of the system. Three main inputs need to be considered to characterise the behaviour of the heat network: the network layout, the characteristics of the network's components, and measurement data of thermodynamic properties during the operation of the network.

The network layout or topology helps to identify the number and physical location of the various components, such as pipes, valves, pumps, heat sources and loads. This is used as the basis for the simulation to provide a visual representation of the main components. In general, a DH network model can be divided into sources, pipes and consumers, in the context of a theoretical representation. To simplify the complexity of the model, in this study the producers and consumers are considered as sources and sinks connected to supply and return pipes.

The next step is to collect information on the characteristics of the network's components and the measured data of thermodynamic properties during the network's operation. The former pertains to the properties of the pipes, which remain constant, while the latter corresponds to the time-varying parameters of the consumers, e.g. heat consumption. Table 1 presents such data.

For the purpose of this analysis, the soil temperature is assumed to be constant over time and for all pipes due to the network's location and structure. Furthermore, all the time-varying parameters are defined at the consumers and at the start of all hydraulically coupled networks (see Section 3.2). One extra parameter is required in order to be use for calibration purposes. In this particular case the supply temperature is selected (Section 3.3), but the return temperature could also be used.

3.2. Simulation tool

There are several frameworks to model a DH network, and the choice depends largely on the purpose of the analysis. In the present work, the Thermal Engineering Systems in Python (TESPy, version 0.7.2 [33]) software is selected to create the underlying network model and run the thermodynamic calculations.

TESPy is an open source framework that provides a powerful simulation toolkit for thermal process engineering, e.g., power plants, district heating systems or heat pumps [30]. With TESPy, it is possible to design plants and simulate stationary operation. The system of equations is solved numerically with an inbuilt solver using the multi-dimensional Newton-Raphson method. To achieve this, the software implements energy and mass balance equations as described in Section 2. In

Table 1
Model parameterisation and calibration information.

Location	Parameter	Symbol
All pipes	aggregated heat transfer coefficient	K
	surrounding temperature	T_{soil}
All consumers	mass flow	$\dot{m}(t)$
	heat demand	$\dot{Q}(t)$
	supply temperature (for calibration)	$T(t)$
Feed-in points and decoupling	Supply flow temperature	$T(t)$

addition, the component-based structure combined with the solution method provides a high degree of flexibility regarding topology and parameterisation.

To build the heat network model, the TESPy documentation [34] provides a list of components which can simulate the real behaviour of the system. The components used for the purpose of this research are described in Table 2.

The construction of the network is the first step to consider when creating a model in TESPy. A general DH network can be divided into three main sections. First, the start and end of the network, represented by the source and sink (Fig. 1-a). Second, a series of repeated connections of pipes and junctions are placed to represent the branches and consumers of the real network topology, as shown in Fig. 1-b/d. Third, the thermal connection to available hydraulically decoupled branches (Fig. 1-c).

Once all components are imported and connected, the system is parameterised at specific locations by using the constant and time-varying physical parameters described in Table 1, which allows to solve the system of equations described in Section 2.

3.3. Model calibration and validation

The effectiveness of mathematical models in analysing existing DH systems largely depends on their ability to accurately replicate observed field conditions [25]. Model calibration for thermal conditions is the procedure of selecting model parameters in order to reduce the deviation between the model's and the observed parameters, e.g., the supply or return temperatures at different points of the network [25].

According to literature [25,28,32], in steady-state thermal modelling of heat networks, the heat transfer coefficient (U in W/m^2 K, see Eq. (5)) is commonly used as a calibration parameter, which provides a benchmark for estimating the deviation of the target parameter and the corresponding calibration. However, the proposed approach considers K, the product of the heat transfer coefficient and the heat transfer area of each pipe, as the calibration parameter in order to deal with the uncertainty of the information of both parameters, previously depicted in Eq. (8).

The present work proposes a calibration method by coupling a multi-objective optimisation technique with a steady-state thermal simulation model. The aim is to find the most suitable values for the aggregated heat transfer coefficient of each pipe in the network (K), thereby minimising the difference between measured and simulated temperatures in each building. This approach has been found to be useful when limited information about the pipes is available. A similar approach was proposed in [25] by applying genetic algorithms to find an appropriate generic heat transfer coefficient for the whole system, but not for each pipe individually. It is worth noting that other methods could have been used without the use of heuristics, such as deterministic minimisation per building, or simply using single-objective optimisation. However, in DH networks, changing the characteristics of a pipe in the model may lead to lower temperature deviations in one building but higher deviations in an adjacent one; therefore, a suitable compromise must be found.

By employing an optimisation approach, the calibration problem is formulated as a nonlinear objective function. Consequently, to reduce the computational effort, this approach can be applied to one branch of the network at a time. This branch-oriented calibration considers the following criteria:

- A decision variable vector $\vec{K}$ containing the aggregated heat transfer coefficient of each available pipe within that branch, and a $\vec{x}$ containing the thermal properties of the network, are passed into the simulation model together.
- The bound constraints are used to set limits on the decision variables of the calibration problem. Since this method assumes that limited information about the pipes is available, a lower bound of 1 W/K and an upper bound of 300 W/K are defined for each element of $\vec{K}$.
- The objective function is defined by Eq. (9), wherein the Root Mean Squared Error formula is employed to minimise the differences between the measured supply temperature and the simulated values of the buildings within the selected branch.
- The simulation period is 12 continuous hours of high demand consumption, whereby assumptions of steady-state conditions is very likely suitable [12].

$$f\left(\vec{K}\right) = RMSE = \sqrt{\frac{1}{n}\cdot\sum_{t=t_1}^{t_n}\left(T_{\mathrm{meas,b},t} - T_{\mathrm{sim,b},t}\right)^2} \tag{9}$$

Fig. 2 depicts the overall branch-oriented calibration method used for this study. In (a), the first branch closer to the starting point of the network is selected (highlighted in light blue). In (b), the proposed thermodynamic model is coupled with the multi-objective optimisation problem. For this, a Non-dominated Sorting GA (NSGA2) algorithm is implemented using the PyGMO scientific optimisation library [35]. The procedure begins by utilizing a random population defined by the decision variable vector $\vec{K}$ and the thermal properties $\vec{x}$, which are imposed on the thermal model. Subsequently, the model solves the system of equations to allow for the calculation of the objective function based on the selected criteria. Next, a new population is generated with the aim of minimising the previously obtained objective function values. These steps are iterated until the stopping criteria is satisfied. And finally, in (c), the selection of the next branch to be optimised begins, considering the already found optimal calibration values of the previous branch (highlighted in grey).

To validate the model, the root mean square error (RMSE) described in Eq. (9) is calculated for all available data of a given time frame.

Table 2
TESPy's representation of real heat network components.

Component	TESPy component
Feed-in point	`Source and Sink`
Consumer	`SimpleHeatExchanger`
Junctions	`Splitter and Merge`
Heat exchanger	`HeatExchanger`
Pipe	`Pipe`
Pumps	`Pump`
Valves	`Valve`

4. Case study: Heat network of DLR site in Lampoldshausen

The "Zero Emission – Hydrogen Site Lampoldshausen" project [36], funded by the Ministry of Economic Affairs, Labour and Tourism of Baden-Württemberg, aims to bring the German Aerospace Center (DLR) test and research site Lampoldshausen closer to becoming a "CO_2-neutral site". In this sense, the heat network used to supply the institute's heat demand has been used as a case study.

4.1. System description

First, the components comprising the heat network are identified and characterized. Two CHP plants serve as the heat source of the network, and their connection to the network (via a heat exchanger) is considered the starting point of the analysed system. In total, 30 buildings are connected to the heat network, of which four are disregarded from the analysis due to their extremely low heat demand and/or infrequent use of the network.

To get a visual representation of the system, all 26 buildings considered are mapped in order to create a network layout. For this purpose, the open licence map OpenStreetMap (OSM) [37] and the folium library [38] are used. As it was not possible to access the original

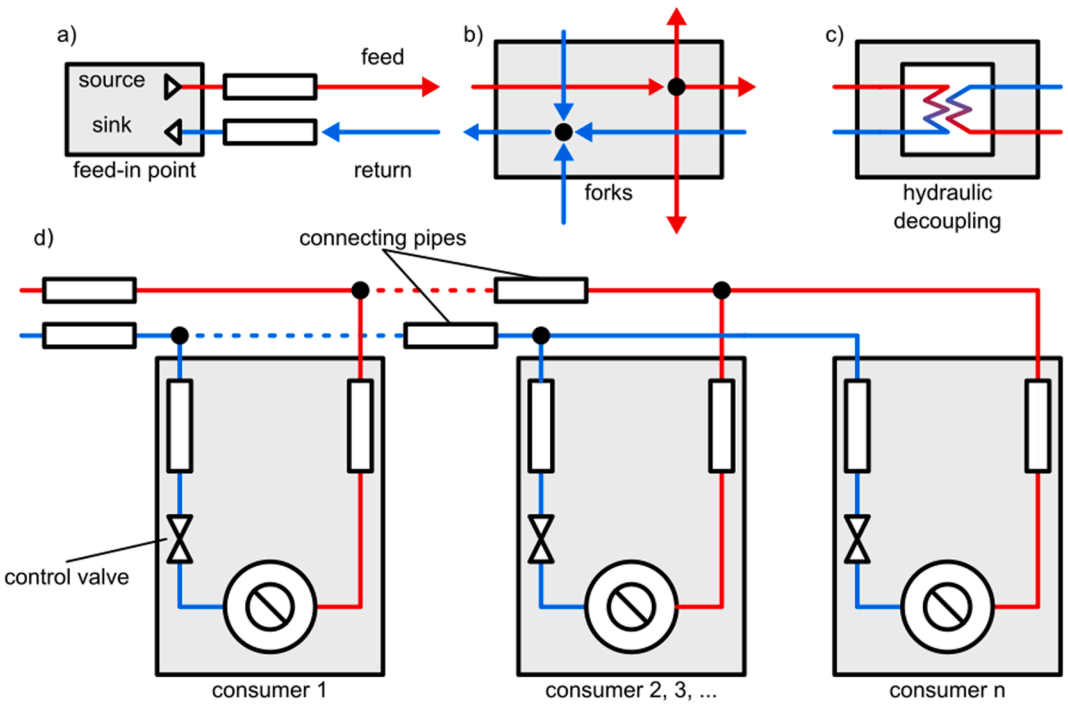

Fig. 1. TESPy components' interconnection for a concrete model representation: a) feed-in point of the network, b) use of a 1-to-n splitter and n-to-1 merger to simulate junctions, c) hydraulic decoupling and d) generic consumer's interconnection.

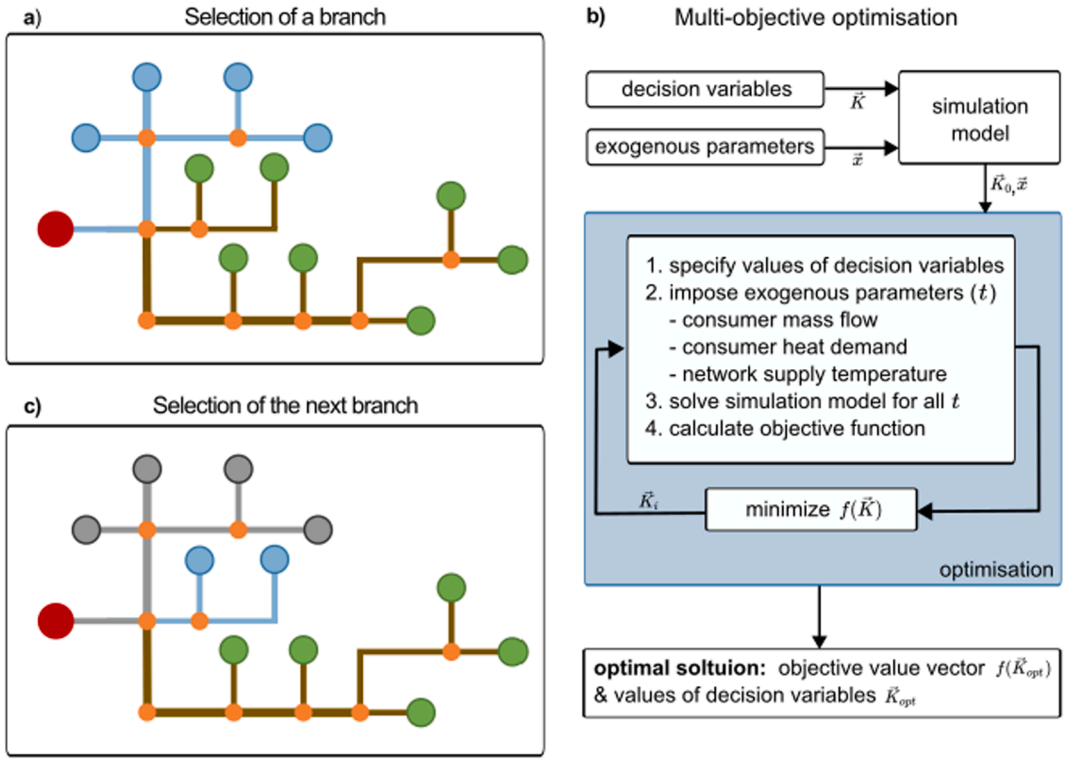

Fig. 2. Abstract representation of the branch-oriented multi-objective calibration method: a) selection of a branch within the system (light blue). b) Multi-objective calibration method. c) selection of the next branch to be calibrated (light blue) considering the previously calibrated valued (grey). (For interpretation of the references to colour in this figure legend, the reader is referred to the web version of this article.)

planning documents of the heat network, some assumptions are made to suggest a piping arrangement and to subsequently determine the length of each pipe. The resulting layout is shown in Fig. 3, where the feed-in point of the network is depicted at the bottom centre of the figure and marked as a red dot. Similarly, the piping arrangement and all the buildings are portrayed. Based on their specific location and distance from the network's starting point, four branches are identified (Fig. 4). The first three branches are hydraulically connected, while the fourth

Fig. 3. Lampoldshausen's heating network layout using OpenSteetMap.

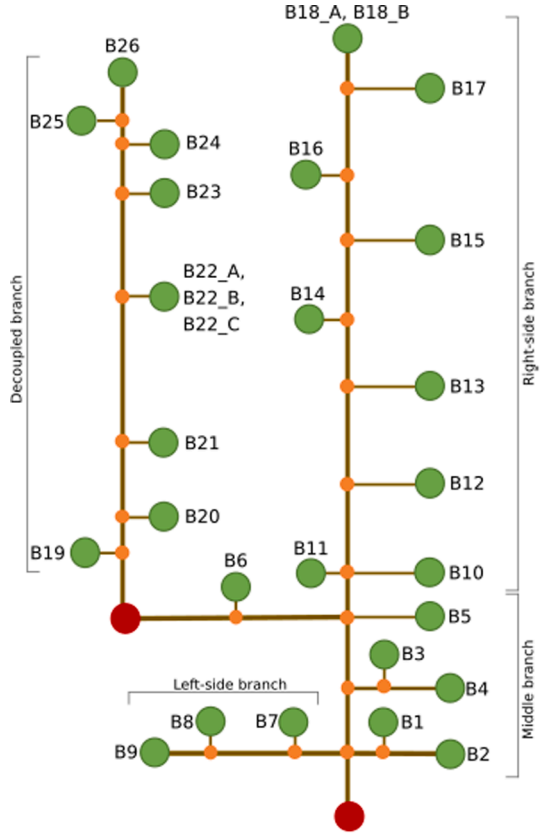

Fig. 4. Lampoldshausen's piping arrangement and identified branches representation (not to scale).

branch is decoupled by the use of a heat exchanger as depicted in both figures.

A total of 53 pipes are presented in Fig. 3. Information on the dimensions of the pipes (i.e., diameters and type of material) is assumed based on the network's topology and internal documentation. The heat transfer coefficient U is obtained from literature review [32]. Table 3 (Supplementary material) summarises all the pipe characteristics used for the uncalibrated model. The soil temperature is assumed to remain constant at a value of 12 °C due to its location. Information provided by site technicians indicates that the heat network is partially installed in large basements and underground areas. The calibration of the network considering a correction of these assumptions is made by using an aggregated heat transfer coefficient K (Section 3.3).

The time-dependent thermal behaviour described in Table 1 was collected through meters installed in all buildings with a 15 min time resolution. This dataset is publicly available. This dataset is publicly available under [39]. During the data analysis, it was found that some buildings have multiple meters installed, monitoring different areas of the building. A total of 36 m were identified, continuously recording thermal data i.e. heat demand, mass flow, and supply and return temperatures. To reduce the number of consumers per building and thus reduce the complexity of the model two strategies are used: (i) if the meters installed in the same building have similar temperature readings, they are merged. This is the case for buildings B1, B5, B10, B13 and B15. (ii) if the temperature difference between two meters in the same building is higher than 3 °C, they are treated as an independent consumer. This is the case for B18 and B22 (Fig. 4). Therefore, a total of 29 consumers are considered for the purpose of this model.

Differences in the supply temperature higher than 3 °C between meters installed at the same physical location or closer are caused by the installation of mixing valves before the meters' locations. As a general rule, the meters were installed upstream of mixing junctions as depicted in Fig. 5-a. However, for four specific consumers (B14, B18_B, B22_B and B22_C), the data was recorded after the mixing Fig. 5-b, where the supply temperature is significantly lower.

To resolve the inconsistency and avoid increasing the complexity of the model, an analytical calculation of adiabatic mixing is used to calculate the pre-mixing temperature and mass flow values and then consider them as the new input parameters. This analytical calculation is based on calculating the incoming mass flow, using the available information after the mixing and assuming that the supply temperature of the consumer is similar to that of the nearest non-mixing consumer. Therefore, by applying Eq. (2) the desired values are obtained.

Additionally, the following steps are carried out for cleaning and preparing of the large dataset used for the analysis:

1. The data was homogenised by setting a common timeindex (in steps of 15 min) for the dataset timeframe: January 2022 for all buildings and interpolating the corresponding values linearly.
2. Due to the limitations of the TESPy simulation tool, a minimum mass flow value was set to avoid convergence problems. The minimum mass flow is 0.01 kg/s.
3. The temperature at the start of the network is assumed based on the temperature of the nearest building (B1) with an additional offset of 0.1 °C. This was assumed due to the lack of a meter installed at the supply temperature delivered by the CHP plants.

The thermal behaviour is plotted to assess the consistency of the data analysis. At the top of Fig. 6, one week of January 2022 is shown to observe temperature variations across the network. It can be observed that the temperature is highest at the consumer closest to the start of the network. Subsequently, a steady decrease is observed depending on the distance and whether the building has a mixing valve or belongs to a hydraulically decoupled branch. This trend highlights the qualitative validation of the measured data. For completeness, the mass flow of the same buildings is presented at the bottom of Fig. 6. The sudden

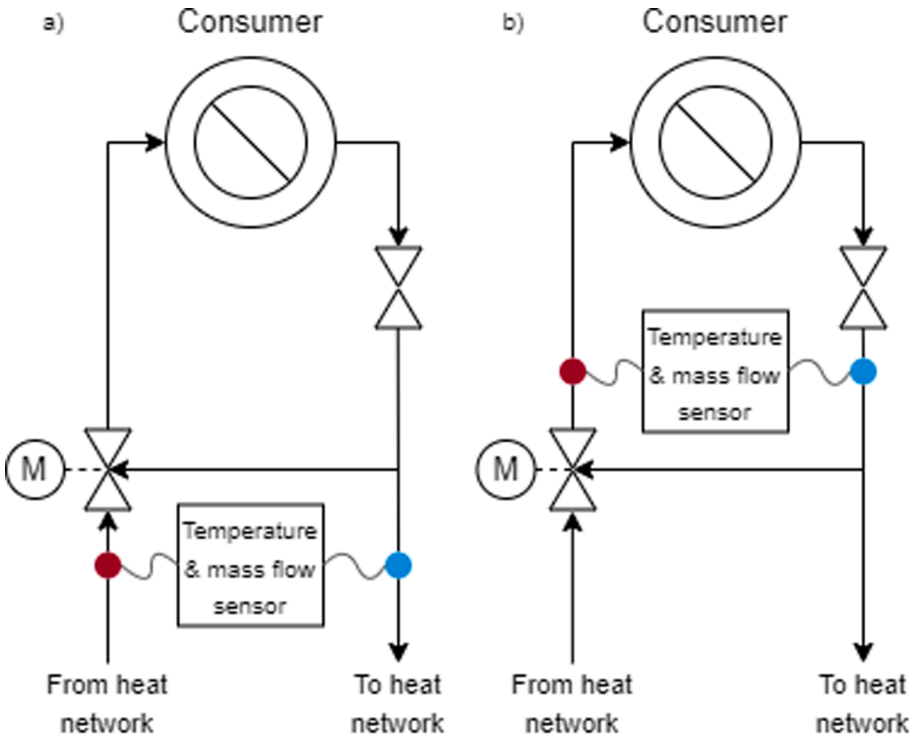

Fig. 5. Mixing valves used at the consumer side: a) Consumer recording thermal behaviour before mixing valve. b) recording thermal behaviour after the mixing.

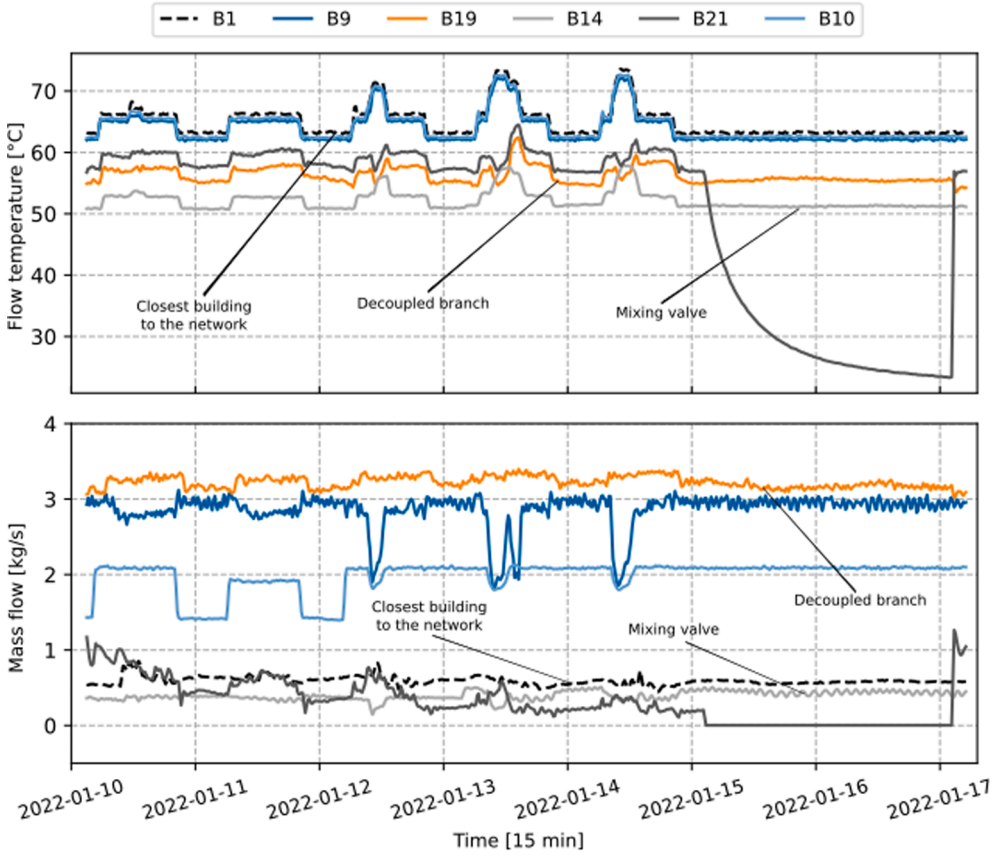

Fig. 6. Variation of temperature and mass flow across the network for multiple buildings: one week of measured data with a 15 min time resolution. In both graphs, it is possible to distinguish the temperature and mass flow of the closest building to the network and observe the effect of temperature drop due to the presence of a hydraulically decoupled branch or the presence of a mixing valve.

temperature drop in B21 can be explained by examining the mass flow behaviour: when there is no mass flow, the temperature will cool down during shutdowns until it reaches an equilibrium with the surrounding temperature or until demand is restored. It is worth noting that shutdowns do not occur for all buildings, and therefore there is continuous heat demand.

5. Results and discussion

A calibrated and validated thermal simulation model for a real DH system was established by using the proposed method. The main results are described in the following section.

5.1. Model validation

The uncalibrated model was compared with the calibrated one using the information from the case study presented in Section 4.1. Results are shown in Fig. 7, depicting the error analysis performed for the month of January 2022, in terms of mean absolute error and RMSE values.

All points below the dotted division line in Fig. 7 indicate the buildings where the calibration of the model decreased the error between the measured data and the simulation, for both the mean absolute error and RMSE. Points above the dotted line indicate an increase of the error in the calibrated model. Results show that for the uncalibrated model, 24.1 % of the measurement points have a mean absolute temperature error less than or equal to 0.5 °C. In contrast, the calibrated model showed that 96.6 % of the points have a mean absolute temperature error less than or equal to 0.5 °C (highlighted area in grey). Due to the use of data from externally installed measuring instruments, the cases of high error values observed after the model's calibration can be attributed to meter-calibration issues. The accuracy of commercial temperature meters varies from ± 0.5 to ± 2.6 °C depending on the brand. In addition, the use of extension wires for distributed control systems (DCS) or programmable logic controllers (PLC) is another source of measurement error [40].

Similar results were found by Wang et al. [25], an absolute temperature error of 0.5 °C to 3 °C for the uncalibrated model and absolute temperature error below 0.6 °C for the calibrated one. It should be noted that in this study the comparison of the measured and simulated data was carried out for only three different thermal conditions compared to the 15 min time resolution dataset used for the present case study. Similarly, [21] presented an absolute temperature error below 1 °C, for a 24 h onsite measurement.

Furthermore, the particular cases where the building's mean absolute temperature error and/or RMSE are significantly high are discussed below:

1. Building B4 was found to have the second lowest mean absolute error before the calibration, but a higher value of 0.43 °C after the calibration. Throughout the data analysis, building B4′s temperature level was constantly only slightly lower than the temperature at the starting point of the network and higher than the temperature of the previous building (B3 – Fig. 4). With a higher distance it is likely to observe higher losses in the network. Therefore, with the lower supply temperature, it can be assumed that the values obtained for this particular building could be erroneous. However, it has been decided to keep this consumer in the model for the sake of transparency and analysis of the measured data.
2. Similarly, building B19 was found to have a lower temperature of approximately 3 °C than the following buildings, e.g., B20, B21 and B22, despite being closer to the starting point of the system.
3. building B21′s RMSE of 1.00 °C after the calibration can be explained by the frequent shutdown of the building at the weekends, also observed in Fig. 6.
4. Finally, it was also found that the high uncalibrated values of B11 can be attributed solely to inaccurate initial assumptions.

5.2. Effect of mass flow regimes

Fig. 8 depicts, on a logarithmic scale, the counts of supply temperature errors for all buildings under different mass flow regimes for the month of January, with data recorded at 15 minutes time resolution.

During the analysis, it was found that the majority of the mass flow data points are between 0.01 kg/s to 2.0 kg/s, and that the total count of temperature error lower than ± 2 °C correspond to 97 % of the data points; proving the effectiveness of the method. This means that once a suitable value for K has been determined using the respective model together with calibration from measurement data, heat losses can also be predicted under different operational conditions, such as lowered supply flow temperature levels in the system and different mass flow

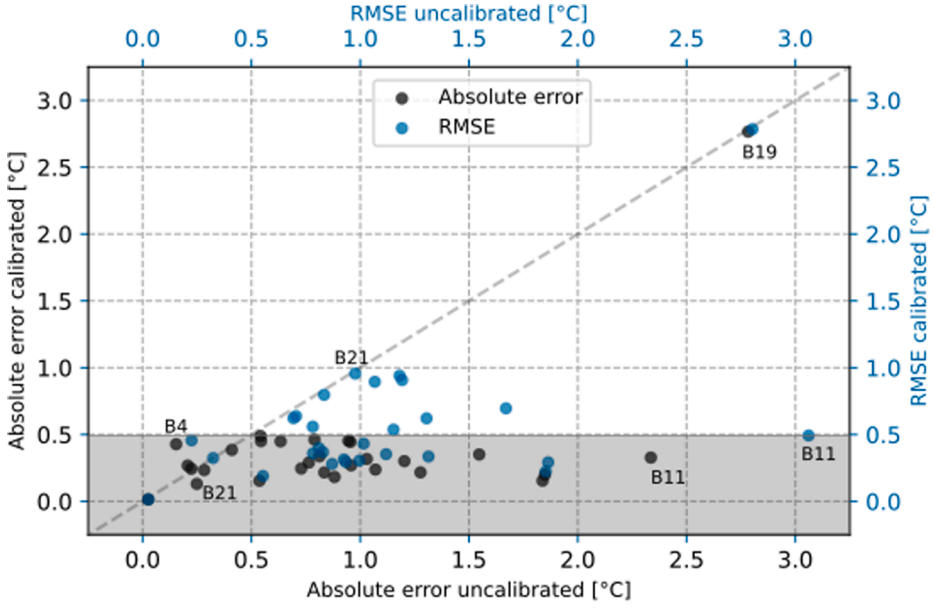

Fig. 7. Comparison of uncalibrated and calibrated model mean absolute error and RMSE for the month of January. The grey area indicates a mean absolute error and RMSE below 0.5 °C in the calibrated model. To facilitate analysis, only certain buildings are labelled.

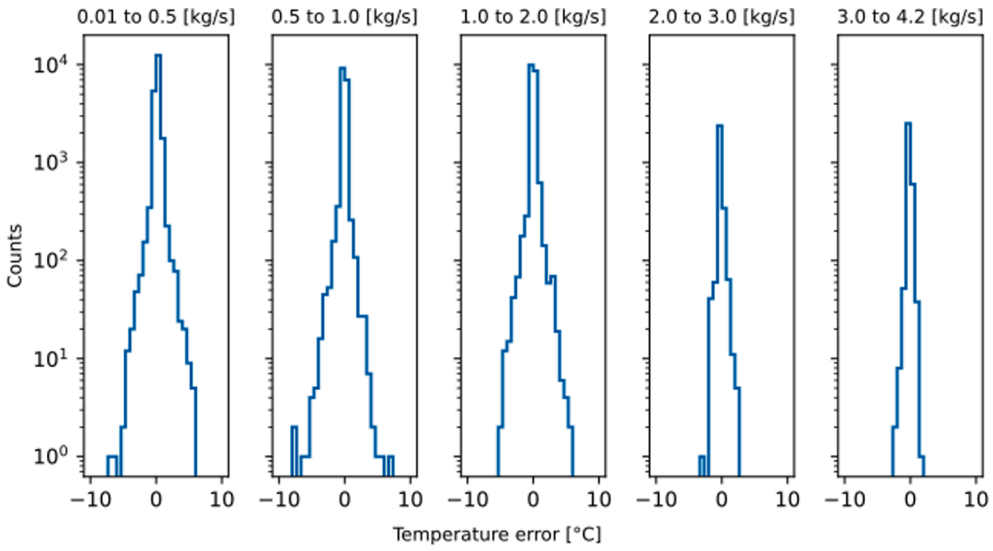

Fig. 8. Logarithmic distribution of the difference between simulated and measured supply temperature at different mass flow regimes for the month of January at 15 minutes time resolution.

regimes. It should be noted, that the heat transfer between a pipe and its surroundings depends on the flow regime inside the pipe and the convection of heat through the pipe and insulation into the soil. One can safely assume that the characteristics of the heat convection do not change if operating conditions change. However, in case the flow regime changes drastically inside the pipes, the approach taken might be erroneous.

Despite the high counts of lower difference between simulated and measured supply temperatures in all flow regimes, it can be observed that with higher mass flows, fewer instances of errors higher than 5 °C occur. This indicated that better predictions of the model are observed. Therefore, in lower the mass flow regimes, it is more likely that neglecting thermal inertia during the calculating the heat losses (Eq. (5)) and the effect of axial heat transfer on the temperature distribution become relevant for the heat losses analysis, as found in [19].

One example of system divergence is presented in Fig. 9, where a sudden reduction of nearly zero mass (B21) flow in the system causes the model to abort calculations after reaching maximum number of iterations, resulting in a high temperature error. Between point A and B, there is a clear sudden drop of the mass flow at building B21, representing a typical demand shutdown over the weekend starting on January 15 and resuming operations on January 17. During this time, the simulated temperature also drops suddenly to its minimum feasible value. This is consistent with the steady-state simulation approach chosen, which disregards the thermal decay processes for the pipe fluid. It is worth mentioning that the reduction of demand in one building does not necessarily affect another building within the same system. As observed in Fig. 9, building B26 continues with a rather steady demand over the same period of time, and the simulated supply temperatures continue to predict its behaviour.

Further development for the presented method is required, such as the option to temporarily disconnect branches of the system when minimal heat demand exists to improve the stability of the model. Additionally, as discussed in this chapter, an adjustment of the K factor could be implemented in variable mass flow regimes. This is because the heat transfer coefficient, among other factors, depends on the flow regime inside the pipes, which may change significantly when mass flow varies by two magnitudes (e.g. from 1 kg/s to 0.01 kg/s).

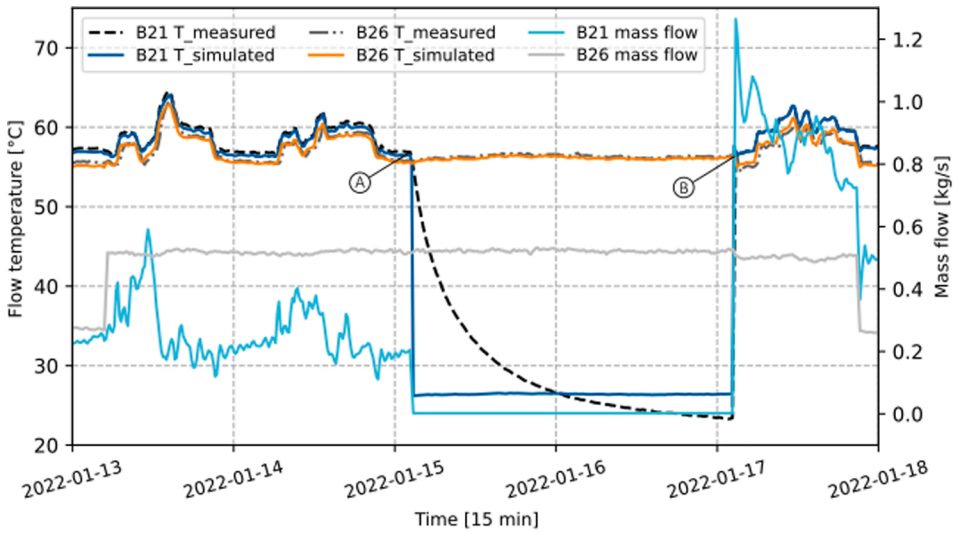

Fig. 9. Uncalibrated and calibrated temperature and mass flow behaviour in buildings B21 and B26. Points (A) and (B) represent the start and end of a shutdown event, respectively.

6. Conclusion and outlook

The present study proposes a method for modelling and calibrating a steady-state heat network using an open-source tool (TESPy) to describe its topology and parameterise it with rather coarse assumptions. Due to the uncertainty associated with such assumptions, the model is calibrated using a heuristic approach (PYGMO), which targets the combination of the heat transfer coefficient and the length of each pipe for calibration. To validate and analyse the method, a heat network in southern Germany with available measured data on the network's thermal behaviour but limited information about the topology and pipe characteristics is utilised.

Results show that after calibration, the mean absolute temperature error between the simulated and measured flow temperatures at all consumers is below 0.5 °C, except in cases of high data uncertainty. These findings clearly indicate the effectiveness and accuracy of the proposed method. Furthermore, it is observed that the model performs better predictions at relatively high mass flow conditions (between 2.0 kg/s to 4.2 kg/s) of individual pipes, but this accuracy decreases at low mass flow conditions (between 0.01 kg/s to 1 kg/s). Consequently, in situations involving changes in network operations (e.g., night shutdowns or setbacks), thermal inertia cannot be reliably predicted.

The obtained results underscore the importance of analysing the operating conditions of the heating network before selecting a suitable modelling approach to assess its performance. While steady-state simulation of a district heating system with highly variable mass flows may lead to deviations in estimating thermal behaviour, it remains as a robust, accurate, and efficient modelling technique for district heating systems operating under relatively constant and design mass flow conditions.

For future work, the thermal inertia component of the thermal analysis could be included whilst keeping the steady-state approach. This could be achieved by implementing a variable heat transfer coefficient depending on the range of the mass flow. Additionally, introducing the possibility of disconnecting buildings from the network topology that are not operational or have minimal heat demand could enhance the stability of the developed system and mitigate convergence problems.

CRediT authorship contribution statement

Diana Maldonado: Writing – review & editing, Writing – original draft, Visualization, Validation, Software, Methodology, Formal analysis, Data curation, Conceptualization. **Patrik Schönfeldt:** Writing – review & editing, Supervision, Methodology, Conceptualization. **Herena Torio:** Writing – review & editing, Supervision, Methodology, Conceptualization. **Francesco Witte:** Writing – review & editing, Visualization, Validation, Supervision, Software, Methodology. **Michael Füting:** Writing – review & editing, Funding acquisition, Conceptualization.

Declaration of competing interest

The authors declare that they have no known competing financial interests or personal relationships that could have appeared to influence the work reported in this paper.

Data availability

The heat-related dataset used for this paper has already been published. Further data will be made available on request.

Acknowledgment

This work was funded by the Baden-Württemberg Ministry of Economic Affairs, Labour and Tourism as part of the "Zero Emission – Hydrogen Site Lampoldshausen" project. We would like to thank the technicians at the German Aerospace Center (DLR) Lampoldshausen site, in particular Tobias Seufert, for their support in collecting the data of the heat network.

Appendix A. Supplementary data

Supplementary data to this article can be found online at https://doi.org/10.1016/j.applthermaleng.2024.123267.

References

[1] IEA - International Energy Agency, Heating overview, (2023). online: https://www.iea.org/reports/heating, accessed 13.02.2024.
[2] Bundesverband der Energie- und Wasserwirtschaft e.V, Publikation entwicklung des wärmeverbrauchs in deutschland, (2022). online: https://www.bdew.de/energie/die-waermeverbrauchsanalyse-des-bdew-ausgabe-2022/, accessed 01/03/2023.
[3] Bundesministerium für Wirtschaft und Energie, Integrierter nationaler energie und klimaplan, (2020). online: https://energy.ec.europa.eu/system/files/2020-06/de_final_necp_main_de_0.pdf, accessed 14/02/2024.
[4] BMWK - Bundesministerium für Wirtschaft und Klimaschutzt, 65 prozent erneuerbare energien beim einbau von neuen heizungen ab 2024 - konzeption zur umsetzung, (2022). https://www.bmwsb.bund.de/SharedDocs/downloads/Webs/BMWSB/584 DE/veroeffentlichungen/bauen/konzeptpapier-65-prozent-ee.585 pdf?_blob=publicationFile&v=5, accessed 14/07/2022.
[5] Der Energieeffizienzverband für Wärme, Kälte und KWK e.V., Haupzbereicht 2021, (2022). online: https://www.agfw.de/zahlen-und-statistiken/agfw-hauptbericht/, accessed 14/07/2022.
[6] E. Commission, D.-G. for Energy, S. Lettenbichler, J. Corscadden, A. Krasatsenka, Advancing district heating & cooling solutions and uptake in european cities – overview of support activities and projects of the european commission on district heating & cooling, Publications Office of the European Union, 2023. DOI: doi/10.2833/51155.
[7] A. Brown, A. Foley, D. Laverty, S. McLoone, P. Keatley, Heating and cooling networks: a comprehensive review of modelling approaches to map future directions, Energy 261 (2022) 125060, https://doi.org/10.1016/j.energy.2022.125060.
[8] AGORA Energiewende, Heat transition 2030 key technologies for reaching the intermediate and long term climate targets in the building sector, (2017). online: https://www.agora-energiewende.de/fileadmin/Projekte/2016/Sektoruebergreifende_EW/Heat-Transition-2030_Summary-WEB.pdf, accessed 17/02/2023.
[9] H. Lund, S. Werner, R. Wiltshire, S. Svendsen, J.E. Thorsen, F. Hvelplund, B. V. Mathiesen, 4th generation district heating (4GDH), Energy 68 (2014) 1–11, https://doi.org/10.1016/j.energy.2014.02.089.
[10] H. Lund, P.A. Østergaard, T.B. Nielsen, S. Werner, J.E. Thorsen, O. Gudmundsson, A. Arabkoohsar, B.V. Mathiesen, Perspectives on fourth and fifth generation district heating, Energy 227 (2021) 120520, https://doi.org/10.1016/j.energy.2021.120520.
[11] M.S. Triebs, E. Papadis, H. Cramer, G. Tsatsaronis, Landscape of district heating systems in germany – status quo and categorization, Energy Convers. Manage.: X 9 (2021) 100068, https://doi.org/10.1016/j.ecmx.2020.100068.
[12] E. Guelpa, Impact of network modelling in the analysis of district heating systems, Energy 213 (2020) 118393, https://doi.org/10.1016/j.energy.2020.118393.
[13] A. Benonysson, Dynamic modelling and operational optimization of district heating systems, (1991).
[14] B. Bøhm, On transient heat losses from buried district heating pipes, Int. J. Energy Res. 24 (2000) 1311–1334.
[15] H.V. Larsen, H. Pálsson, B. Bøhm, H.F. Ravn, Aggregated dynamic simulation model of district heating networks, Energ. Conver. Manage. 43 (2002) 995–1019, https://doi.org/10.1016/S0196-8904(01)00093-0.
[16] H.V. Larsen, B. Bøhm, M. Wigbels, A comparison of aggregated models for simulation and operational optimisation of district heating networks, Energ. Conver. Manage. 45 (2004) 1119–1139, https://doi.org/10.1016/j.enconman.2003.08.006.
[17] I. Gabrielaitiene, B. Bøhm, B. Sunden, Modelling temperature dynamics of a district heating system in naestved, denmark—a case study, Energ. Conver. Manage. 48 (2007) 78–86, https://doi.org/10.1016/j.enconman.2006.05.011.
[18] V.D. Stevanovic, B. Zivkovic, S. Prica, B. Maslovaric, V. Karamarkovic, V. Trkulja, Prediction of thermal transients in district heating systems, Energ. Conver. Manage. 50 (2009) 2167–2173, https://doi.org/10.1016/j.enconman.2009.04.034.
[19] B. van der Heijde, M. Fuchs, C. Ribas Tugores, G. Schweiger, K. Sartor, D. Basciotti, D. Müller, C. Nytsch-Geusen, M. Wetter, L. Helsen, Dynamic equation-based thermo-hydraulic pipe model for district heating and cooling systems, Energ. Conver. Manage. 151 (2017) 158–169, https://doi.org/10.1016/j.enconman.2017.08.072.
[20] K. Sartor, P. Dewalef, Experimental validation of heat transport modelling in district heating networks, Energy 137 (2017) 961–968, https://doi.org/10.1016/j.energy.2017.02.161.

[21] H. Wang, H. Meng, T. Zhu, New model for onsite heat loss state estimation of general district heating network with hourly measurements, Energ. Conver. Manage. 157 (2018) 71–85, https://doi.org/10.1016/j.enconman.2017.11.062.
[22] P. Wallentén, Steady-state heat loss from insulated pipes, Byggnadsfysik LTH, Lunds Tekniska Högskola, 2016.
[23] J. Duquette, A. Rowe, P. Wild, Thermal performance of a steady state physical pipe model for simulating district heating grids with variable flow, Appl. Energy 178 (2016) 383–393, https://doi.org/10.1016/j.apenergy.2016.06.092.
[24] B. van der Heijde, A. Aertgeerts, L. Helsen, Modelling steady-state thermal behaviour of double thermal network pipes, Int. J. Therm. Sci. 117 (2017) 316–327, https://doi.org/10.1016/j.ijthermalsci.2017.03.026.
[25] J. Wang, Z. Zhou, J. Zhao, A method for the steady-state thermal simulation of district heating systems and model parameters calibration, Energ. Conver. Manage. 120 (2016) 294–305, https://doi.org/10.1016/j.enconman.2016.04.074.
[26] J. Röder, B. Meyer, U. Krien, J. Zimmermann, T. Stührmann, E. Zondervan, Optimal design of district heating networks with distributed thermal energy storages – method and case study, Int. J. Sustain. Energy Plann. Manage. 31 (2021) 5–22, https://doi.org/10.5278/ijsepm.6248.
[27] A. Hussein, A. Klein, Modelling and validation of district heating networks using an urban simulation platform, Appl. Therm. Eng. 187 (2021) 116529, https://doi.org/10.1016/j.applthermaleng.2020.116529.
[28] L. Vorspel, J. Bücker, District-heating-grid simulation in python: DiGriPy, Computation 9 (2021) 72, https://doi.org/10.3390/computation9060072.
[29] M. Wirtz, nPro: A web-based planning tool for designing district energy systems and thermal networks, Energy 268 (2023) 126575, https://doi.org/10.1016/j.energy.2022.126575.
[30] F. Witte, I. Tuschy, TESPy: Thermal Engineering Systems in Python, J. Open Source Software 5 (2020) 2178, https://doi.org/10.21105/joss.02178.
[31] D. Lohmeier, D. Cronbach, S.R. Drauz, M. Braun, T.M. Kneiske, Pandapipes: An open-source piping grid calculation package for multi-energy grid simulations, Sustainability 12 (2020), https://doi.org/10.3390/su12239899.
[32] T. Nussbaumer, S. Thalmann, A. Jenni, J. Ködel, Handbook on Planning of District Heating Networks, Swiss Federal Office of Energy, Bern, 2020.
[33] F. Witte, TESPy: Thermal engineering systems in Python. Version v0.6.2, (2022). DOI: 10.5281/zenodo.2555866.
[34] F. Witte, TESPy: Thermal Engineering Systems in Python, (2023). online: https://tespy.readthedocs.io, accessed 14/07/2023.
[35] F. Biscani, D. Izzo, A parallel global multiobjective framework for optimization: pagmo, J. Open Source Software 5 (2020) 2338, https://doi.org/10.21105/joss.02338.
[36] DLR - Institute of Networked Energy Systems, Zero emission – hydrogen site lampoldshausen research project, (2023). online: https://www.dlr.de/ve/en/desktopdefault.aspx/tabid-16122/26109_read-67236/, accessed 17/02/2023.
[37] OpenStreetMap, (2023). online: https://www.openstreetmap.org.
[38] R. Story, Folium, (2022). online: https://pypi.org/project/folium/.
[39] D. Maldonado, P. Schönfeldt, M. Füting, Temperature, water velocity and heat consumption of a heat network in southern, Germany. Zenodo (Oct. 24, 2023), https://doi.org/10.5281/zenodo.10036105.
[40] G. Prentice, Temperature measurement accuracy guidelines, (2015). online: https://www.piprocessinstrumentation.com/instrumentation/temperature-measurement, accessed 17/05/2023.